Synthesis of three-revolute spatial chains for body guidance

Jonathan D. Hauenstein[a], Charles W. Wampler[b], Martin Pfurner[c]

[a] *University of Notre Dame, Notre Dame, IN, USA*
[b] *General Motors R & D, Warren, MI, USA*
[c] *University of Innsbruck, Innsbruck, Austria*

Abstract

For a given mechanism type, the solution set of a body guidance synthesis problem comprises all mechanisms whose end-effector can reach a set of prescribed poses (position and orientation). For three-revolute spatial chains, five general poses will yield a synthesis problem having only finitely many solutions, while specifying fewer than five poses leads to higher-dimensional solution sets. We use numerical algebraic geometry to compute solution sets for two to five general poses, and in particular, we find, for the first time, that the five-pose synthesis problem generically has 456 solutions. We also show how our results agree with and extend results in the literature.

Keywords: Kinematics, mechanism synthesis, body guidance, numerical algebraic geometry, polynomial continuation

1. Introduction

The problem of synthesizing mechanisms that guide their end-effector through a number of prescribed discrete poses (position and orientation) has a long tradition in kinematics with the some of the first formulations and solutions by Schoenflies [1] and Burmester [2]. Beginning in the second half of the 20$^{\text{th}}$ century, various planar and spatial synthesis problems were formulated, e.g., see [3], with McCarthy [4] providing a good general overview.

Whereas a six degree-of-freedom robot, such as a serial-link six-revolute (6R) arm or a Stewart-Gough parallel-link robot (i.e., type 6(SPS)),[1] can

[1] We use the usual notations for joint types: "R" for revolute, "P" for prismatic, and

carry a payload through an arbitrary number of poses within its reachable workspace, mechanisms with fewer degrees of freedom also have many uses. Since a lower-degree-of-freedom device cannot reach arbitrary poses, one approach to designing such mechanisms is to specify a finite number of poses that must be reached and then solving the associated kinematics equations to find mechanisms that can reach those poses.

In this paper, we consider the synthesis of serial three-revolute (3R) spatial chains. A simple dimension count indicates that five is the maximum number of general end-effector poses for which a solution will exist. Thus, we consider the synthesis problems arising from 2, 3, 4, and 5 prescribed general poses and solve them using numerical algebraic geometry. For 5 general poses, the synthesis problem has a finite number of solutions whereas fewer poses yield an infinite number, i.e., a positive-dimensional solution set.

While a 3R synthesis problem might arise out of the desire to use a 3R robot for a task, a method of solving such problems has many other potential uses. As an example, consider guiding body B with respect to body A using a one degree-of-freedom mechanism through 5 poses. One option is to use a spatial 3-loop mechanism that connects B to A via one 3R chain and two S-S pairs. It has been shown, e.g., see [5, 6], that can construct S-S pairs for motion through up to 7 poses. Combining two such S-S pairs with a solution to the 3R synthesis problem gives the complete synthesis of the mechanism. One could consider many other arrangements that include a 3R chain.

Previous work on the 3R synthesis problem has been published by Lee and Mavroidis [7, 8, 9], also with Merlet in [10]. For the 3-pose and 4-pose cases, they restrict to problems having a finite solution set by fixing certain design parameters: six parameters for the 3-pose case and three parameters for the 4-pose case. The resulting synthesis equations were solved using either homotopy continuation [7, 8] or elimination methods [9]. Whereas those efforts used the polynomial nature of the equations to compute complete solution sets using complex numbers, the 5-pose case was treated in [10] by using interval analysis to find all solutions in a specified interval box for one particular 5-pose synthesis problem.

These prior publications all formulate the synthesis problems as a system of polynomial equations arising from a matrix equation using the Denavit and Hartenberg [11] convention of modeling spatial linkages. We develop

"S" for spherical.

an alternative formulation, more amenable to numerical solution, based on a direct determination of the location of the joint axes. This allows us to solve the 3- and 4-pose problems in a more general way, without resorting to pre-specifying mechanism parameters, and to completely solve the 5-pose problem in the complex domain. We describe the relationship between the two formulations and replicate the earlier results with this new formulation.

Our general solutions in the complex domain allow us to efficiently carry out subsequent calculations by the methods of parameter continuation and regeneration, which we also describe. In our computations, we use the software package `Bertini` [12]. For more information about using homotopy continuation and numerical algebraic geometry applied to kinematics, see Wampler and Sommese [13] and Sommese, Verschelde and Wampler [14].

The remainder of the paper is as follows. Section 2 presents our reformulation of 3R synthesis as a system of polynomial equations. We briefly review numerical algebraic geometry in Section 3 and describe its use in Section 4, to completely solve the synthesis problems of 3R spatial chains for 2, 3, 4, and 5 general poses. We apply the methods to solve numerical examples in Section 5. A discussion about the results and conclusion of this paper are presented in Section 6.

2. Problem Formulation

We begin by reviewing the Denavit-Hartenberg (D-H) conventions for modeling a serial-link chain. The works of Lee and Mavroidis on 3R synthesis were formulated in terms of a product of transformation matrices populated by D-H parameters, including joint angles. We start with the same underlying link geometry, but eschew joint angles and instead use joint vectors that directly indicate the linkage conformation at each specified pose.

Denavit-Hartenberg parameters describe the relative positions of two arbitrary lines in space, see Figure 1, which will be the axes of adjacent revolute joints in a serial chain. Two coordinate frames Σ and Σ' are attached to the two lines such that the z-axis of Σ is aligned with the first line and the x-axis is parallel to their common normal. Coordinate frame Σ' has its origin at the footpoint of the common normal on the second line, with its z-axis aligned with this line and its x-axis aligned with the x-axis of Σ. Parameter a denotes the distance between the lines, d is the offset of the common normal on the first line to the origin of Σ and α is the twist angle. The relative transformation from Σ to Σ' can be written as consecutive transformations of the form:

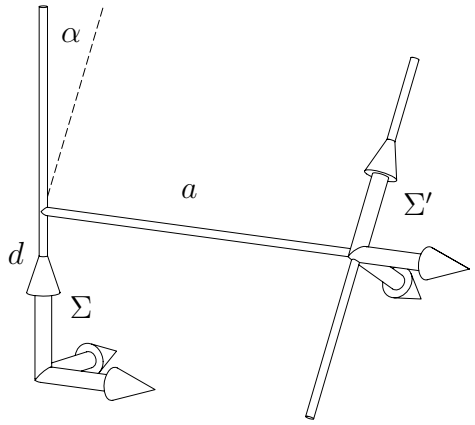

Figure 1: Denavit-Hartenberg parameters

translation along the z-axis with distance d, followed by a translation along x-axis with distance a, and then a rotation around x-axis by an angle α.

When the D-H convention is used for the description of a serial chain with n revolute joints, one is able to write the pose of the end effector frame Σ_{n+1} with respect to the base frame Σ_0 in terms of relative transformations from Σ_i to Σ_i' together with, for each $i = 1, \ldots, n$, a transformation from Σ_{i-1}' to Σ_i that is a rotation around z-axis i by joint angle θ_i. For a fully general chain, one must also include angle θ_0 as a mechanism parameter associated to the placement of the mechanism in the world frame and parameters θ_{n+1} and d_{n+1} associated to the placement of the end-effector frame in the final link. Altogether, there are $3n + 6$ mechanism parameters, namely

$$\theta_0, \{(d_i, a_i, \alpha_i), i = 0, \ldots, n\}, \theta_{n+1}, d_{n+1}$$

and there are n joint angles, θ_i, $i = 1, \ldots, n$. For N general poses and an n-revolute chain, the synthesis problem has $3n+6+Nn$ unknowns and $6N$ constraints. In particular, these are equal when $n = 3$ and $N = 5$. For comparison to the work of Lee and Mavroidis on 3R problems, we note that they rename the last two parameters as $\phi = \theta_4$ and $d = d_4$.

From this point forward, we focus our discussion on 3R spatial chains, i.e., $n = 3$, with N given poses. For $i = 1, \ldots, N$, let pose i be given by its translational part $\mathbf{p}_i \in \mathbb{R}^3$ and rotational part $\mathbf{R}_i \in SO(3)$ with respect to the base frame. The kinematic chain in pose i is shown in Fig. 2.

We construct a system of synthesis equations by using a slight modification of the formulation in Wampler and Morgan [15] for solving the inverse

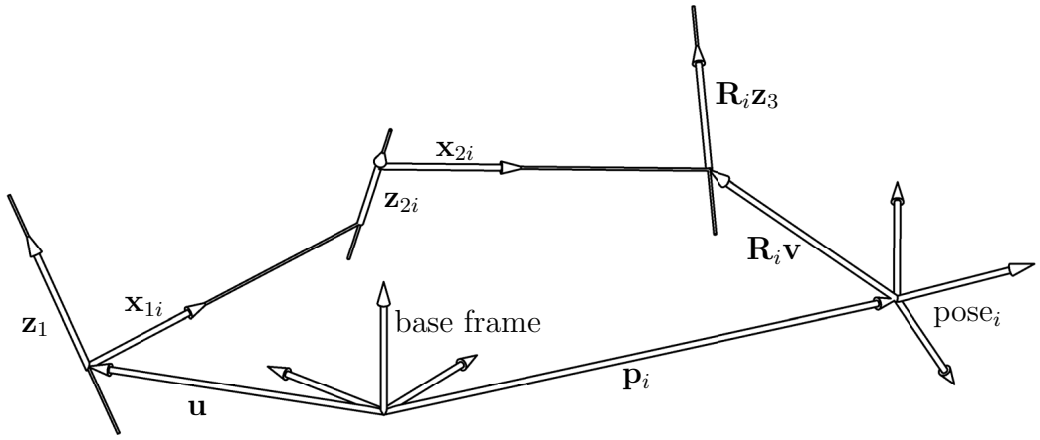

Figure 2: Kinematic chain in pose i

kinematics of serial 6R spatial chains. Since the first joint axis is fixed in the base frame, let $\mathbf{z}_1$ denote the (unknown) unit vector directed along the first joint axis. Similarly, since the third joint axis is fixed in the the end-effector frame, let $\mathbf{z}_3$ denote the (unknown) unit vector directed along the third joint axis in the end-effector frame. Thus, for pose i, $\mathbf{R}_i\mathbf{z}_3$ is the unit vector directed along the third joint axis in the base frame. Also, for each pose i, let $\mathbf{z}_{2i}$ denote the (unknown) unit vector directed along the second joint axis in the base frame.

Assuming that none of the axes are parallel, which will be true for solutions of the synthesis problem for general poses, the unit vectors along the common normals of the axes are

$$\mathbf{x}_{1i} = \frac{1}{\sin\alpha_1}\mathbf{z}_1 \times \mathbf{z}_{2i}, \qquad \mathbf{x}_{2i} = \frac{1}{\sin\alpha_2}\mathbf{z}_{2i} \times \mathbf{R}_i\mathbf{z}_3, \tag{1}$$

where α_j denotes the twist angle between axes j and $j+1$ for $j = 1, 2$.

Let $\mathbf{u}$ denote the vector pointing from the origin of the base frame to the foot point of the common normal between axis one and axis two on axis one. Similarly, let $\mathbf{v}$ denote the vector in the end-effector frame pointing from its origin to the foot point of the common normal between axis two and axis three on axis three. In the base frame, this vector is $\mathbf{R}_i\mathbf{v}$ as shown in Fig. 2. Our computations will use $\mathbf{u}$ and $\mathbf{v}$ as variables in the synthesis problem. Later, to confirm the results of Lee and Mavroidis, we will write these in terms of D-H parameters.

Using as variables $\mathbf{u}$, $\mathbf{v}$, and the joint axis vectors, namely $\mathbf{z}_1$, $\mathbf{z}_3$, and

$(\mathbf{z}_{2i}, i = 1, \ldots, N)$, the remaining (unknown) design parameters are link lengths a_1 and a_2, offset d_2, and twist angles α_1 and α_2. For each pose $i = 1, \ldots, N$, these must satisfy the loop closure vector equation

$$\mathbf{u} + \frac{a_1}{\sin(\alpha_1)}\mathbf{z}_1 \times \mathbf{z}_{2i} + d_2\mathbf{z}_{2i} + \frac{a_2}{\sin(\alpha_2)}\mathbf{z}_{2i} \times \mathbf{R}_i\mathbf{z}_3 = \mathbf{p}_i + \mathbf{R}_i\mathbf{v}, \tag{2}$$

while the definition of a twist angle implies

$$\begin{aligned} \mathbf{z}_1 \cdot \mathbf{z}_{2i} &= \cos\alpha_1, \\ \mathbf{z}_{2i} \cdot \mathbf{R}_i\mathbf{z}_3 &= \cos\alpha_2. \end{aligned} \tag{3}$$

Additionally, the joint axis vectors must all be unit length.

Instead of imposing unit-length conditions on the joint axis vectors, we introduce new non-unit vectors aligned with the joint axes. Assuming that the values d_2, $\sin\alpha_1$, and $\sin\alpha_2$ are all nonzero, which is the case for general poses, we can define the vectors

$$\mathbf{w}_1 := \frac{a_1}{d_2\sin(\alpha_1)}\mathbf{z}_1, \qquad \mathbf{w}_3 := \frac{a_2}{d_2\sin(\alpha_2)}\mathbf{z}_3, \tag{4}$$

$$\mathbf{w}_{2i} := d_2\mathbf{z}_{2i}, \quad i = 1, \ldots, n, \tag{5}$$

with which we rewrite Eq. (2) as

$$\mathbf{u} + \mathbf{w}_1 \times \mathbf{w}_{2i} + \mathbf{w}_{2i} + \mathbf{w}_{2i} \times \mathbf{R}_i\mathbf{w}_3 = \mathbf{p}_i + \mathbf{R}_i\mathbf{v}, \quad i = 1, \ldots, N. \tag{6}$$

We can eliminate $\mathbf{u}$ as follows. Consider the vector function

$$\mathbf{f}(\mathbf{w}_1, \mathbf{w}_2, \mathbf{w}_3, \mathbf{v}, \mathbf{p}, \mathbf{R}) = \mathbf{w}_1 \times \mathbf{w}_2 + \mathbf{w}_2 + \mathbf{w}_2 \times \mathbf{R}\mathbf{w}_3 - \mathbf{p} - \mathbf{R}\mathbf{v}. \tag{7}$$

Then, Eq. (6) is equivalent to

$$\mathbf{u} = -\mathbf{f}(\mathbf{w}_1, \mathbf{w}_{2i}, \mathbf{w}_3, \mathbf{v}, \mathbf{p}_i, \mathbf{R}_i), \quad i = 1, \ldots, N \tag{8}$$

so that

$$\mathbf{f}(\mathbf{w}_1, \mathbf{w}_{21}, \mathbf{w}_3, \mathbf{v}, \mathbf{p}_1, \mathbf{R}_1) = \mathbf{f}(\mathbf{w}_1, \mathbf{w}_{2i}, \mathbf{w}_3, \mathbf{v}, \mathbf{p}_i, \mathbf{R}_i), \quad i = 2, \ldots, N. \tag{9}$$

Since the link lengths a_1 and a_2, the link twists α_1 and α_2, and link offset d_2 are independent of i, we additionally have for $i = 2, \ldots, N$:

$$\begin{aligned} \mathbf{w}_1 \cdot \mathbf{w}_{21} &= \mathbf{w}_1 \cdot \mathbf{w}_{2i}, \\ \mathbf{w}_{21} \cdot \mathbf{R}_1\mathbf{w}_3 &= \mathbf{w}_{2i} \cdot \mathbf{R}_i\mathbf{w}_3, \\ \mathbf{w}_{21} \cdot \mathbf{w}_{21} &= \mathbf{w}_{2i} \cdot \mathbf{w}_{2i}. \end{aligned} \tag{10}$$

For $N \geq 2$, the resulting system Eqs. (9) and (10) consist of $6(N-1)$ quadratic equations in $9+3N$ unknowns, which are the three coordinates each for the vectors $\mathbf{w}_1$, $\mathbf{w}_3$, $\mathbf{v}$, and $\mathbf{w}_{2i}$, $i = 1, \ldots, N$. Comparing the number of unknowns to the number of equations, for $N \geq 2$, the dimension of the solution set for N general poses is $3(5-N)$. Hence, $N = 5$ defines a system of 24 quadratic equations in 24 unknowns which has a zero-dimensional solution set, i.e., finitely many solutions.

2.1. Backsolving

After solving the system consisting of Eqs. (9) and (10), one can recover the description of the serial chain in terms of its link parameters. First, Eq. (8) directly yields $\mathbf{u}$, while Eqs. (4) and (5) imply the following formulas for the unit direction vectors along the axes and the offset on the second axis:

$$\mathbf{z}_1 = \frac{\mathbf{w}_1}{||\mathbf{w}_1||}, \quad \mathbf{z}_{21} = \frac{\mathbf{w}_{21}}{||\mathbf{w}_{21}||}, \quad \mathbf{z}_3 = \frac{\mathbf{w}_3}{||\mathbf{w}_3||}, \quad d_2 = \mathbf{z}_{21} \cdot \mathbf{w}_{21}. \tag{11}$$

Using Eq. (3), the twist angles can be computed via

$$\alpha_1 = \arccos(\mathbf{z}_1 \cdot \mathbf{z}_{21}), \qquad \alpha_2 = \arccos(\mathbf{z}_{21} \cdot \mathbf{R}_1 \mathbf{z}_3). \tag{12}$$

Finally, from Eq. (4), we recover the link lengths via

$$a_1 = d_2 \sin\alpha_1 \mathbf{w}_1 \cdot \mathbf{z}_1, \qquad a_2 = d_2 \sin\alpha_2 \mathbf{w}_3 \cdot \mathbf{z}_3. \tag{13}$$

We note that this backsolving procedure does not yield a unique set of D-H parameters as each direction vector $\mathbf{z}_1$, $\mathbf{z}_{21}$, and $\mathbf{z}_3$ and the twist angles can be negated. These choices result in compatible changes in the signs of the link lengths and the link offset, but do not change the underlying geometry of the 3R mechanism. That is, each solution in the variables $(\mathbf{w}_1, \mathbf{w}_{21}, \mathbf{w}_3, \mathbf{v})$ represents a unique 3R mechanism even though the corresponding D-H parameters have several arbitrary choices of signs.

This backsolving procedure can run into trouble if any of α_1, α_2, d_2, a_1, or a_2 are equal to zero. This is not of concern if the given poses are general, but it could be a problem for special poses.

3. Numerical Algebraic Geometry

Every equation in the system (9,10) is a polynomial. Numerical algebraic geometry is a collection of algorithms for finding and manipulating

the solutions of such systems. Let $z \in \mathbb{C}^n$ be a set of n unknowns and let $F(z) = \{f_1(z), \ldots, f_m(z)\} : \mathbb{C}^n \to \mathbb{C}^m$ be a set of m polynomial functions in z. Suppose $m = n$, in which case one usually expects the set of solutions to the system $F(z) = 0$ to consist of a finite number of isolated points. Polynomial continuation, as developed primarily in the 1980s, finds all isolated roots of such a system by creating a start system $G(z) = 0$ and a homotopy function $H(z, t)$, where t is a new variable. The polynomial systems G and H are constructed to match the structure of F in a way that guarantees that $G(z) = 0$ has at least as many isolated solutions as $F(z) = 0$ and that starting at the solutions of $G(z) = 0$, the system $H(z, t) = 0$ has smooth paths progressing monotonically with t to the roots of F. One then finds the roots of F by tracking these paths numerically. As described in [16], a re-issue of Morgan's 1987 book, the homotopy function is usually of the form

$$H(z, t) = F(z)(1 - t) + \gamma t G(z) = 0,$$

where choosing γ as a random complex number ensures, with probability one, the smoothness of the solution paths for $0 < t \leq 1$.

Numerical algebraic geometry builds on basic polynomial continuation to also treat cases where the solution set has components that are positive dimensional, i.e., curves, surfaces, etc., which is always the case when $m < n$ and may happen for $m \geq n$ if the equations are not general. Systems having solution components of several different dimensions can also be solved. To find a solution component, say $S \subset \mathbb{C}^n$, of dimension k, the essential maneuver is to append to $F(z)$ an additional k linear equations, say $L(z) = \{\ell_1(z), \ldots, \ell_k(z)\} = 0$ where the coefficients in L have been chosen as random complex numbers. Then, with probability one, among the set of all isolated solutions of the "sliced" system $\{F(z), L(z)\} = 0$ there is a subset, say W, that are in S, and the number of these points is equal to the degree of S. The set W is called a *witness point set*, and the ordered collection $\mathcal{W} = \{F, L, W\}$ is a *witness set* for S. Since we are once again in the position of finding isolated roots, traditional polynomial continuation can be employed although more advanced techniques are often more efficient. In any case, once a witness set has been found, the slices can be moved based on input parameters to yield solutions of interest as demonstrated in Sections 5.2 and 5.3. The component can also be sampled by moving the coefficients of L, and one can do many other operations, such as intersecting the component with other algebraic sets. A full exposition of the fundamentals of numerical algebraic geometry can be found in [17] while [12] describes more recent

developments along with details of how to use the software package `Bertini` to do calculations.

Suppose, as above, that $S \subset \mathbb{C}^n$ has dimension k and we slice it down to isolated points by intersecting it with k linear equations, $L(z) = 0$. Instead of using general linear equations, which are functions of all n coordinates of z, suppose we intersect it with special ones that depend only on $r < n$ of the coordinates. An extreme example is a linear equation in just one variable, say $\ell(z) = z_1 - a = 0$, for some constant a. This fixes z_1 and effectively removes that variable from the equations, which can have the effect of lowering the degree of the system. For example, the equation $xy - 1 = 0$ describes a hyperbola, a quadratic algebraic set. The intersection of this hyperbola with a general line in (x, y) yields two points, where 2 is equal to the degree of the polynomial $xy - 1$. In contrast, the intersection with the vertical line $x - a = 0$ for $a \neq 0$ gives just one point, namely $(x, y) = (a, 1/a)$.

For another example, consider the pair of quadratic equations

$$F(x, y, z) = \{xy - z, xz - y^2\} = 0, \tag{14}$$

whose solution is the twisted cubic, $C = \{(x, y, z) = (t, t^2, t^3) \mid t \in \mathbb{C}\}$ and the line $\{(x, y, z) = (t, 0, 0) \mid t \in \mathbb{C}\}$. Intersecting C with a general plane gives three points, but intersecting it with a linear function of just (x, y) gives only two points. This reflects the fact that although C is a degree 3 curve, its projection onto the (x, y)-plane is the parabola $y = x^2$, a mere quadric. In general, intersecting a k-dimensional algebraic set $S \subset \mathbb{C}^n$ with k linear equations involving only $r < n$ of the variables but otherwise general gives a pseudowitness point set for the projection of S onto those r coordinates, and that projection may have a lower degree than S itself. (For further discussion of projections in numerical algebraic geometry, see [18] and [12, Ch. 16].)

These observations are made to clarify the relation between the results of this paper and the prior work on the 3R synthesis problem. Given $N \leq 5$ general poses, the solution set has dimension $3(5 - N)$, i.e., it is six-dimensional for $N = 3$ and three-dimensional for $N = 4$. In [7, 9], the $N = 3$ problem is reduced to one having a finite number of roots by fixing six link parameters. Similarly, in [8], three link parameters are fixed. (In both [7, 8], two variants are considered, picking different parameters to fix.) As just discussed, fixing a variable is equivalent to intersecting the solution set with a special linear equation, a coordinate-aligned hyperplane.

In contrast, instead of using specially aligned linear equations, we will compute a witness set for the positive-dimensional solution set by intersect-

ing it with the appropriate number of *general* linear equations. These linear equations can subsequently be specialized in a homotopy to fix any subset of the variables; having computed the witness set, we will be prepared to apply numerical algebraic geometry to perform many other operations. In particular, since Section 2.1 shows that $(\mathbf{w}_1, \mathbf{w}_{21}, \mathbf{w}_3, \mathbf{v})$ represents a unique 3R spatial chain, we will specialize to general linear equations involving just the variables $(\mathbf{w}_1, \mathbf{w}_{21}, \mathbf{w}_3, \mathbf{v})$. This gives a pseudowitness set, say $\widehat{\mathcal{W}} = \{F, \widehat{L}, \widehat{W}\}$, for this projection that can be used in further computations, where $\widehat{L}$ is a set of general linear equations in $(\mathbf{w}_1, \mathbf{w}_{21}, \mathbf{w}_3, \mathbf{v})$ and $\widehat{W}$ is the set of solutions to system $\{F, \widehat{L}\} = 0$.

One powerful technique for performing further computations is *regeneration* [19]. For example, suppose that for $N = 3$ or 4 poses, one wishes to fix certain D-H parameters as was done in [7, 8, 9]. One might make the same choices as in one of those papers, but any other choice can be accommodated by our approach as well. To simplify the discussion, we assume for the moment that the number of parameters to fix is exactly the number required to reduce the problem to a finite number of isolated solutions. For brevity, let us introduce $q := (\mathbf{w}_1, \mathbf{w}_{21}, \mathbf{w}_3, \mathbf{v})$ to denote the subset of variables used in the projection. Since each point q represents a unique 3R spatial chain, fixing D-H parameters is equivalent to imposing a set of algebraic conditions on these variables, say $\widehat{F}(q) = 0$. If the new equations were linear, say $\widehat{M}(q) = 0$, then one may find the solutions using the homotopy $H(t) = \{F, t\widehat{L} + (1-t)\widehat{M}\} = 0$ starting at $t = 1$ from the solution points $\widehat{W}$ for $\{F, \widehat{L}\} = 0$ and tracking solution paths as $t \to 0$. In the case of fixing D-H parameters, however, the entries in $\widehat{F}(q)$ can have degree larger than one, and we need a start system $\widehat{G}(q)$ whose degrees match it, so that the homotopy $H(t) = \{F, t\widehat{G} + (1-t)\widehat{F}\} = 0$ will have solution paths leading to all the solutions of $\{F, \widehat{F}\} = 0$. For this purpose, it suffices for each entry in $\widehat{G}$ to be a product of linear factors in q, the number of factors matching the degree of the corresponding entry in $\widehat{F}$. Choosing one factor in each polynomial of $\widehat{G}$ results in a system of the form $\{F, \widehat{L}_j\} = 0$ to solve, where index j ranges over all possible ways of choosing the factors. Since we can solve each of these, the total solution set for $\{F, \widehat{G}\} = 0$ can be assembled as a union of their solutions, and we are then ready to proceed to solve $\{F, \widehat{F}\} = 0$. We leave the precise details of regeneration to the references [19] and [12, Ch. 12]. The key point of this discussion is that once a pseudowitness set is on hand for the projection onto variables q, one is ready to solve a wide

range of problems related to 3R synthesis, including all the ones treated by Lee and Mavroidis, as described below.

Finally, we note that once a general example[2] for a problem with isolated roots has been solved, the isolated roots of any other problem of that type can be computed very efficiently by *parameter continuation*. In 3R synthesis, this applies to the 5-pose problem or to any 3-pose or 4-pose problem having the requisite number of link parameters pre-specified. One merely forms a homotopy that moves the pose data and pre-specified link parameters continuously from the general example to the target example and follows paths from the solution points for the general example to those of the target. Once the solution set for the general example is in hand, it no longer matters how many homotopy paths were tracked to find it: all future problems in the class are solved by tracking just the root count number of paths. To be concrete, we find that the 5-pose problem has in general 456 isolated solutions. Although we track many more than that number to find this, once the first complete solution set is in hand, all isolated solutions to any other 5-pose 3R synthesis problem can be solved by tracking just 456 paths. We give examples of this below.

4. General Solving

With the formulation from Section 2 and using numerical algebraic geometry as summarized in Section 3, we are able to solve the synthesis problems for 3R spatial chains. In Table 1, we summarize the dimension and degree of the solution set for $N = 2, \ldots, 5$ general poses in all of variables used, namely $(\mathbf{w}_1, \mathbf{w}_{21}, \ldots, \mathbf{w}_{2N}, \mathbf{w}_3, \mathbf{v})$, as well as in only the variables $(\mathbf{w}_1, \mathbf{w}_{21}, \mathbf{w}_3, \mathbf{v})$, these being sufficient to define a unique 3R mechanism. In particular, Table 1 shows that the 3R synthesis problem for 5 general poses has 456 solutions. It remains an open question to determine if all 456 solutions can be real.

We note that in the $N = 4$ and $N = 5$ cases, there are several degenerate components for which either $\mathbf{w}_1$ or $\mathbf{w}_3$ is zero. We ignore these components and do not count them in the degree table.

As outlined in Section 3, each entry in Table 1 corresponds to a witness or pseudowitness set, which enables subsequent computations via regeneration or parameter homotopy. In particular, by tracking 456 solutions paths in

[2] "General example" means all pre-specified parameters are chosen at random in complex Euclidean space.

Table 1: Dimension and degree of 3R synthesis solution sets for N general poses.

	$(\mathbf{w}_1, \mathbf{w}_{21}, \ldots, \mathbf{w}_{2N}, \mathbf{w}_3, \mathbf{v})$		$(\mathbf{w}_1, \mathbf{w}_{21}, \mathbf{w}_3, \mathbf{v})$	
N	Dimension	Degree	Dimension	Degree
2	9	63	9	35
3	6	1704	6	672
4	3	6612	3	3132
5	0	456	0	456

a parameter homotopy, one is able to compute all isolated solutions to any 5-pose synthesis problem as will be illustrated in Section 5.1. Moreover, by using regeneration, one may solve any version of the 3- or 4-pose problems treated by Lee and Mavroidis [7, 8, 9], as we shall do in Sections 5.2 and 5.3.

When we solve a *general* problem, the pose data is picked by a random number generator as are certain other quantities, such as the coefficients of the general linear equations used for slicing out a witness set. Since the correctness of our answers are subject to some uncertainty due to the interplay between random number generation, numerical round-off, and various tolerance settings, it is advisable to perform certain checking procedures. The simplest approach is to run each problem several times with new random numbers and confirm that the results are consistent. To be even more confident, we can validate aspects of the computation. Section 4.1 describes using α-theory to prove that the numerically computed points actually correspond to distinct solutions. Section 4.2 then uses trace test computations to verify the degrees presented in Table 1.

4.1. Validation using alpha-theory

Let $F(z)$ be a system of n polynomials in n unknowns z. A natural question when using numerical computations is to decide how accurate one needs to numerically represent the solutions. For nonsingular solutions, i.e., for $\xi \in \mathbb{C}^n$ such that $F(\xi) = 0$ and rank $JF(\xi) = n$ where $JF(z)$ is the $n \times n$ Jacobian matrix of $F(z)$, one approach is to make this decision based on the quadratic convergence basin of Newton's method surrounding ξ. A sufficient condition that a given point lies in the quadratic convergence basin of some solution is provided by α-theory [20] (see also [21, Ch. 8]) and can be tested locally at the given point. In short, α-theory relies upon the fact that a point

is in the quadratic convergence basin of Newton's method associated with some nonsingular solution if the Newton residual is small compared with a condition number based on the higher order derivatives of F at the point.

The software package `alphaCertified` [22] uses α-theoretic tools to decide which points are certifiably in distinct quadratic convergence basins of Newton's method thereby corresponding to distinct solutions. When the polynomial system $F(z)$ has real coefficients, it can also certifiably categorize each corresponding solution as real or nonreal as described in [22]. In all of the examples presented in Section 5, the *a posteriori* validation using `alphaCertified` took less time than the path tracking using `Bertini`.

4.2. Validation using trace test

The trace test derived in [23], which can be efficiently computed via [24], is a method for verifying that a collection of solutions form a witness point set thereby validating degrees of components. The underlying foundation is to consider the centroid of the paths which arise by intersecting a component with a family of parallel slices. As shown in [23], one has a valid witness point set for a component if and only if as the slice moves parallel to itself the centroid of the corresponding paths moves linearly.

To illustrate this, reconsider the hyperbola A defined by $xy - 1 = 0$. For simplicity, consider intersecting A with the family of slices defined by

$$L(x, y; t) = 3x + 2y - t = 0.$$

As t varies, this line moves parallel to itself and its intersection with A defines 2 solution paths, namely

$$\left(\frac{t}{6} + \frac{\sqrt{t^2 - 24}}{6}, \frac{t}{4} - \frac{\sqrt{t^2 - 24}}{4}\right) \quad \text{and} \quad \left(\frac{t}{6} - \frac{\sqrt{t^2 - 24}}{6}, \frac{t}{4} + \frac{\sqrt{t^2 - 24}}{4}\right).$$

Clearly, each path is not linear in t. However, the centroid of the two paths:

$$\left(\frac{t}{6}, \frac{t}{4}\right),$$

is indeed linear in t thus confirming $\deg A = 2$.

The `Bertini` software package always performs the trace test when computing witness sets for positive-dimensional sets. This serves to verify the results for $N = 2, 3, 4$ in the left-hand column of Table 1. In addition, when

using slices that only involve a subset of the variables, one must consider the trace test only in the coordinates of the centroid which involve those variables. This variant of the trace test verified the results for $N = 2, 3, 4$ in the right-hand column of Table 1.

For the $N = 5$ case, whose solution set consists of finitely many points, there is no higher-dimensional set to slice, so a modification of the trace test is needed. As proposed in [25], the key maneuver is to create a problem that has a positive-dimensional solution set by allowing one or more of its fixed parameters to vary. One then may perform a multihomogeneous trace test in which slices respect the distinction between the original variables and the parameters that became variables. Specifically, in our test, we let the third coordinate of $\mathbf{p}_5$, denoted $\mathbf{p}_5^{(3)}$, be a free variable, where $\mathbf{p}_5$ is the position vector for the fifth pose. This gives a system with a one-dimensional solution set. We slice it with an equation of the form

$$L_1(\mathbf{w}_1, \mathbf{w}_{21}, \ldots, \mathbf{w}_{25}, \mathbf{w}_3, \mathbf{v}) \cdot L_2(\mathbf{p}_5^{(3)}) = t$$

where L_1 and L_2 are general linear functions in their respective variables. As t varies, the trace test showed that there are now 5556 paths, with 5100 satisfying $L_1 = 0$ and 456 satisfying $L_2 = 0$ at $t = 0$ thereby confirming the result for $N = 5$ in Table 1.

5. Examples

In the following, we utilize the setup described above to solve various problems involving the synthesis of 3R spatial chains. All computations were performed using `Bertini` [12] and `alphaCertified` [22] running on 2.4 GHz Opteron 6378 processors with 64-bit Linux and 128 GB of memory.

5.1. 5-pose problem

Lee, Mavroidis, and Merlet [10] use interval methods to compute solutions to a 5-pose synthesis problem. They report that 5 days of computations on a cluster yielded 6 real solutions inside their search domain and 20 real solutions outside. Their approach was guaranteed to find all solutions inside the search domain, with no guarantee about what it would find outside that domain. We will consider this problem using a parameter homotopy that tracks 456 solution paths and finds all solutions.

To facilitate the parameter homotopy, we represent matrices in $SO(3)$ using quaternions. Accordingly, our parameter space is a linear space of

dimension $5(4+3) = 35$ (five poses, each having four quaternion coordinates and three position coordinates). To get the count of 456 solutions for 5-poses as reported in Section 4, we solved the system for five general poses. With those solutions in hand, we take a parameter homotopy defined by the straight line between our general 5 poses and the following 5 poses from [10] in quaternion form:

$$
\begin{aligned}
\mathbf{q}_1 &= [\ -0.3938225625 \quad 0.1584268617 \quad -0.7620982874 \quad 0.4888874299\ ],\\
\mathbf{q}_2 &= [\ -0.4982569794 \quad -0.6821984629 \quad -0.1514278639 \quad -0.5132395558\ ],\\
\mathbf{q}_3 &= [\ 0.2880644106 \quad -0.7219903545 \quad 0.07665279784 \quad -0.6243982478\ ],\\
\mathbf{q}_4 &= [\ 0.5848734779 \quad -0.1591869762 \quad 0.5080877441 \quad -0.6119063374\ ],\\
\mathbf{q}_5 &= [\ -0.08487799894 \quad -0.4692735393 \quad 0.4400168937 \quad -0.7608963161\ ],\\
\mathbf{p}_1 &= [\ 8.310644971 \quad -1.993959918 \quad 4.52564663\ ],\\
\mathbf{p}_2 &= [\ 8.46243208 \quad 3.909344844 \quad 3.781393231\ ],\\
\mathbf{p}_3 &= [\ 8.213357066 \quad 4.720930002 \quad 1.906020548\ ],\\
\mathbf{p}_4 &= [\ 6.61008808 \quad -0.9786178219 \quad 7.933012701\ ],\\
\mathbf{p}_5 &= [\ 7.498628082 \quad -2.362107226 \quad -0.5803329915\ ].
\end{aligned}
$$

The 456 paths were tracked in approximately 3 minutes using a single processing core (3 seconds when using 64 cores) and validated using `alphaCertified` as discussed in Section 4.1 to show that this synthesis problem has 28 real solutions and 428 nonreal solutions. Upon backsolving for the D-H parameters, we find the 26 real solutions reported in [10] plus two others. Numerical approximations of these two additional solutions are shown in Table 2 in the variables of this article and in Table 3 in D-H parameters.

	solution 27	solution 28
$\mathbf{v}$	$[-9.1211, -63.1593, 11.2619]$	$[0.2905, 2.9166, -5.1925]$
$\mathbf{w}_1$	$[-6.7541, -10.6480, -7.7532]$	$[-0.4602, -0.3576, 0.2614]$
$\mathbf{w}_{21}$	$[-0.4275, 3.2653, -4.2770]$	$[9.2547, -7.6281, -3.2358]$
$\mathbf{w}_{22}$	$[-4.4717, 2.9986, -0.3877]$	$[10.7207, -6.1127, 1.4178]$
$\mathbf{w}_{23}$	$[-4.8099, 1.5482, 1.8989]$	$[8.2235, -7.7296, -5.1900]$
$\mathbf{w}_{24}$	$[-4.0426, -0.1579, 3.5735]$	$[9.2516, -7.6290, -3.2424]$
$\mathbf{w}_{25}$	$[-3.9427, 3.4069, -1.4092]$	$[6.9043, -7.4587, -7.1419]$
$\mathbf{w}_3$	$[11.1844, -0.3805, 0.2417]$	$[-0.0113, 0.0734, 0.1121]$

Table 2: Two additional real solutions for the 5-pose problem from [10]

5.2. 4-pose problems

To synthesize mechanisms to reach 4 general poses, Lee and Mavroidis [8] consider two different ways of fixing three D-H parameters, thereby defining

	solution 27	solution 28
θ_0	-0.5653	-0.9102
α_0	2.1221	1.1491
α_1	1.5548	1.8751
α_2	1.5848	0.5460
α_3	1.5492	0.5849
$\phi = \theta_4$	1.6048	-0.1522
a_0	12.2344	-11.9659
a_1	79.8919	7.5699
a_2	60.4154	0.8676
a_3	-63.4329	-0.7294
d_0	89.4297	-1.7058
d_1	44.8209	1.3618
d_2	5.3979	12.4221
d_3	6.9700	-5.1415
$d = d_4$	-11.4125	9.4792

Table 3: D-H parameters for the two additional real solutions for the 5-pose problem from [10] (angles in radians)

problems having finitely many solutions. Both formulations fix α_0 and θ_0, whereas the first way fixes a_0 and the second way fixes d_0. Each choice gives 36 solutions.

To address these same problem specifications using our choice of variables, we begin by expressing $\mathbf{z}_1$ and $\mathbf{u}$ in terms of D-H parameters:

$$\mathbf{z}_1 = \begin{bmatrix} \sin\alpha_0 \sin\theta_0 \\ -\sin\alpha_0 \cos\theta_0 \\ \cos\alpha_0 \end{bmatrix} \quad \text{and} \quad \mathbf{u} = \begin{bmatrix} a_0\cos\theta_0 + d_1 \sin\alpha_0 \sin\theta_0 \\ a_0 \sin\theta_0 - d_1 \sin\alpha_0 \cos\theta_0 \\ d_0 + d_1 \cos\alpha_0 \end{bmatrix}.$$

Since $\mathbf{w}_1$ points in the direction of $\mathbf{z}_1$, fixing α_0 and θ_0 to general values imposes the following two linear conditions:

$$\begin{bmatrix} \cos\theta_0 & \sin\theta_0 & 0 \\ \cos\alpha_0 & 0 & -\sin\alpha_0 \sin\theta_0 \end{bmatrix} \mathbf{w}_1 = 0. \tag{15}$$

One can directly deform two of the general linear slices involving the variables $\mathbf{w}_1, \mathbf{w}_{21}, \mathbf{w}_3, \mathbf{v}$ to these two slices, leaving the third unchanged. Tracking the 3132 paths (see Table 1, line $N = 4$) of this homotopy yields 242 non-degenerate isolated solutions.

That takes care of the first two D-H parameters, α_0 and θ_0. In the first set up of Lee and Mavroidis, the third parameter to be fixed is a_0. This introduces the constraint

$$\left[\begin{array}{ccc} \cos\theta_0 & \sin\theta_0 & 0 \end{array}\right] \mathbf{u} - a_0 = 0. \tag{16}$$

Since $\mathbf{u}$ is quadratic in the variables $\mathbf{w}_1, \mathbf{w}_{21}, \mathbf{w}_3, \mathbf{v}$, we must first regenerate [19] a quadratic starting polynomial to match it. We do this starting from the solution set found in the previous paragraph and now moving the third linear slice to a new general position, generating a second solution set of size 242. Combining these two gives a quadratic polynomial (the product of two linears) and 484 solution point (the union of the two solution sets). Deforming the quadratic to (16) constitutes a homotopy with 484 paths that 36 solutions. This is in agreement with [8].

The second setup of Lee and Mavroidis fixes d_0 instead of a_0. This leads to replacing (16) with the constraint

$$\left[\begin{array}{ccc} \cos\alpha_0 \sin\theta_0 & -\cos\alpha_0 \cos\theta_0 & -\sin\alpha_0 \end{array}\right] \mathbf{u} + \sin\alpha_0 d_0 = 0, \tag{17}$$

which is again a quadratic. We place this as the target of the final homotopy preceding, and again the 484 paths lead to 36 solutions as in [8].

We note that with this setup, each new instance of these synthesis problems can now be solved using a parameter continuation that tracks only 36 paths. As an illustration, we consider the numerical example in [8] which fixes the second set of parameters, namely

$$d_0 = -5,\ \alpha_0 = 0.6435011,\ \text{and}\ \theta_0 = 0.3947911.$$

Lee and Mavroidis report the average time to compute the 36 solutions as 33 days. As in Section 5.1, we utilized a quaternion representation for matrices in $SO(3)$ with the following 4 poses from [8]:

$$\begin{array}{l}
\mathbf{q}_1 = \left[\begin{array}{cccc} -0.03360779745 & -0.6915500603 & -0.7212239947 & 0.02156338409 \end{array}\right], \\
\mathbf{q}_2 = \left[\begin{array}{cccc} 0.4774989481 & -0.8512909324 & -0.106624952 & -0.1895511079 \end{array}\right], \\
\mathbf{q}_3 = \left[\begin{array}{cccc} -0.1874552152 & 0.8351297956 & 0.3625630704 & -0.3687367445 \end{array}\right], \\
\mathbf{q}_4 = \left[\begin{array}{cccc} 0.643435552 & -0.3641213401 & -0.5763108741 & -0.3482414629 \end{array}\right], \\
\mathbf{p}_1 = \left[\begin{array}{ccc} -0.2446998 & 4.946913 & 4.610238 \end{array}\right], \\
\mathbf{p}_2 = \left[\begin{array}{ccc} 12.06793 & 5.833343 & 3.247047 \end{array}\right], \\
\mathbf{p}_3 = \left[\begin{array}{ccc} 9.567735 & 8.133992 & 3.10951 \end{array}\right], \\
\mathbf{p}_4 = \left[\begin{array}{ccc} 3.660175 & 1.031613 & 7.988142 \end{array}\right].
\end{array}$$

We note that this setup corrects a typo in the $(1,2)$ entry of the rotation matrix $\mathbf{R}_1$ from [8] — it should be .9989744. In our experiment, the tracking

of the 36 paths required 4 seconds using a single processing core. Validating the results using `alphaCertified` yielded 8 real and 28 nonreal solutions as reported in [8]. Table 4 lists the real solutions using the variables of this article which correspond to the real solutions presented in [8, Table 1] using D-H parameters.

Solution	$\mathbf{v}$	$\mathbf{w}_1$	$\mathbf{w}_{21}$	$\mathbf{w}_3$
1	$\begin{bmatrix} -3.0988 \\ 3.6612 \\ -0.41177 \end{bmatrix}$	$\begin{bmatrix} 0.98076 \\ -2.3538 \\ 3.4000 \end{bmatrix}$	$\begin{bmatrix} 1.2760 \\ -1.1048 \\ 1.0729 \end{bmatrix}$	$\begin{bmatrix} 0.77205 \\ 2.6470 \\ -1.4706 \end{bmatrix}$
2	$\begin{bmatrix} -5.6285 \\ -0.51606 \\ -0.15248 \end{bmatrix}$	$\begin{bmatrix} 0.15952 \\ -0.38285 \\ 0.55300 \end{bmatrix}$	$\begin{bmatrix} 3.7433 \\ 0.94592 \\ 6.5842 \end{bmatrix}$	$\begin{bmatrix} 0.84557 \\ -0.17929 \\ -1.1483 \end{bmatrix}$
3	$\begin{bmatrix} 4.0551 \\ 27.174 \\ -1.0552 \end{bmatrix}$	$\begin{bmatrix} 0.082364 \\ -0.19767 \\ 0.28553 \end{bmatrix}$	$\begin{bmatrix} 75.543 \\ 108.23 \\ -131.48 \end{bmatrix}$	$\begin{bmatrix} 0.015603 \\ 0.073782 \\ -0.0001514 \end{bmatrix}$
4	$\begin{bmatrix} -0.27820 \\ 6.6037 \\ -0.30204 \end{bmatrix}$	$\begin{bmatrix} 0.40533 \\ -0.9728 \\ 1.4052 \end{bmatrix}$	$\begin{bmatrix} 5.4343 \\ 2.2961 \\ -0.099582 \end{bmatrix}$	$\begin{bmatrix} 0.19194 \\ 1.5229 \\ -0.26632 \end{bmatrix}$
5	$\begin{bmatrix} -14.338 \\ 6.7435 \\ -6.5585 \end{bmatrix}$	$\begin{bmatrix} 0.25753 \\ -0.61807 \\ 0.89276 \end{bmatrix}$	$\begin{bmatrix} -2.1813 \\ 1.8668 \\ 2.9063 \end{bmatrix}$	$\begin{bmatrix} -1.1822 \\ -2.4120 \\ -1.4908 \end{bmatrix}$
6	$\begin{bmatrix} 2.0137 \\ 14.238 \\ -3.6496 \end{bmatrix}$	$\begin{bmatrix} 0.090172 \\ -0.21641 \\ 0.31259 \end{bmatrix}$	$\begin{bmatrix} 6.2732 \\ 4.0777 \\ 1.8517 \end{bmatrix}$	$\begin{bmatrix} -0.39455 \\ -1.4309 \\ 0.89787 \end{bmatrix}$
7	$\begin{bmatrix} -5.8114 \\ 9.6122 \\ 1.4676 \end{bmatrix}$	$\begin{bmatrix} -0.13027 \\ 0.31265 \\ -0.45160 \end{bmatrix}$	$\begin{bmatrix} 6.9366 \\ 3.9225 \\ -0.51028 \end{bmatrix}$	$\begin{bmatrix} 1.1200 \\ 0.29303 \\ 0.25628 \end{bmatrix}$
8	$\begin{bmatrix} -5.0094 \\ -1.3690 \\ -0.028369 \end{bmatrix}$	$\begin{bmatrix} 0.11031 \\ -0.26473 \\ 0.38239 \end{bmatrix}$	$\begin{bmatrix} 1.8348 \\ 1.8555 \\ 7.6947 \end{bmatrix}$	$\begin{bmatrix} 0.79594 \\ -0.31294 \\ -0.84242 \end{bmatrix}$

Table 4: Real solutions for the 4-pose problem from [8] numbered as in [8, Table 1]

5.3. 3-pose problems

In [7, 9], to address the case of 3 general poses, Lee and Mavroidis consider two different ways of fixing six D-H parameters generally to yield finitely many solutions. Both fix a_0, d_0, α_0, and θ_0, with the first fixing a_1 and d_1, and the second fixing $d = d_4$ and $\phi = \theta_4$. Each choice results in 8 solutions.

In the first case, the vector $\mathbf{u}$ is known which yields three quadratic equations in $\mathbf{w}_1, \mathbf{w}_{21}, \mathbf{w}_3, \mathbf{v}$. The vector $\mathbf{z}_1$ is also known yielding the two linear constraints in Eq. (15) together with the quartic constraint

$$\|\mathbf{w}_1\|^2(\|\mathbf{w}_{21}\|^2 - (\mathbf{z}_1 \cdot \mathbf{w}_{21})^2) - a_1^2 = 0.$$

Using regeneration [19] starting from the witness set computed in Section 4 with general slices in $\mathbf{w}_1, \mathbf{w}_{21}, \mathbf{w}_3, \mathbf{v}$, our approach verifies the results in [7, 9] that this synthesis problem generically has 8 solutions.

We can now use parameter continuation to track 8 solution paths to solve instances of this synthesis problem, which in the examples tested took about one second using a single processing core. For example, [9] considers fixing

$$a_0 = -2,\ d_0 = -4,\ \alpha_0 = 0.9272952180,\ \theta_0 = -0.6435011088,\ a_1 = 2,\ d_1 = -2.$$

Using quaternions, the 3 poses are

$$\begin{array}{l}
\mathbf{q}_1 = \left[\begin{array}{cccc} 0.006527140016 & 0.8963938272 & 0.1653542019 & 0.4112097893 \end{array}\right], \\
\mathbf{q}_2 = \left[\begin{array}{cccc} 0.9012958544 & -0.35536808 & -0.08755445437 & -0.2317617918 \end{array}\right], \\
\mathbf{q}_3 = \left[\begin{array}{cccc} 0.3838000391 & 0.8510348734 & -0.07509131152 & -0.3504261251 \end{array}\right], \\
\mathbf{p}_1 = \left[\begin{array}{ccc} 2.1230391 & 4.5332828 & -6.8794793 \end{array}\right], \\
\mathbf{p}_2 = \left[\begin{array}{ccc} -3.0281379 & 4.4823767 & 3.0253581 \end{array}\right], \\
\mathbf{p}_3 = \left[\begin{array}{ccc} -4.4258684 & 1.6855691 & -5.2240167 \end{array}\right].
\end{array}$$

The validation of the solutions using `alphaCertified`, shows this problem has 4 real and 4 nonreal solutions verifying [9]. Table 5 lists the real solutions using the variables of this article which correspond to the real solutions presented in [9, Table 1] using D-H parameters.

Solution	$\mathbf{v}$	$\mathbf{w}_1$	$\mathbf{w}_{21}$	$\mathbf{w}_3$
1	$\begin{bmatrix} 1.8225 \\ 2.9391 \\ -4.7929 \end{bmatrix}$	$\begin{bmatrix} 0.41724 \\ 0.55632 \\ -0.52155 \end{bmatrix}$	$\begin{bmatrix} -0.51154 \\ 0.22856 \\ 2.8868 \end{bmatrix}$	$\begin{bmatrix} -0.011012 \\ -0.016837 \\ -0.012494 \end{bmatrix}$
2	$\begin{bmatrix} 0.96665 \\ 3.3693 \\ -4.7659 \end{bmatrix}$	$\begin{bmatrix} -0.39060 \\ -0.52080 \\ 0.48825 \end{bmatrix}$	$\begin{bmatrix} 1.3533 \\ -1.8394 \\ 1.8981 \end{bmatrix}$	$\begin{bmatrix} -0.14264 \\ -0.22997 \\ -0.38769 \end{bmatrix}$
3	$\begin{bmatrix} 1.8462 \\ 2.0000 \\ -6.2308 \end{bmatrix}$	$\begin{bmatrix} -0.80000 \\ -1.0667 \\ 1.0000 \end{bmatrix}$	$\begin{bmatrix} 0.19200 \\ -1.744 \\ 0.96000 \end{bmatrix}$	$\begin{bmatrix} 0.92308 \\ -1.0341 \cdot 10^{-7} \\ 0.38462 \end{bmatrix}$
4	$\begin{bmatrix} 0.68041 \\ 2.1330 \\ -6.6324 \end{bmatrix}$	$\begin{bmatrix} -1.1642 \\ -1.5522 \\ 1.4552 \end{bmatrix}$	$\begin{bmatrix} -0.58069 \\ -1.8703 \\ 0.76160 \end{bmatrix}$	$\begin{bmatrix} 1.3884 \\ -0.055464 \\ 0.16352 \end{bmatrix}$

Table 5: Real solutions for the 3-pose problem from [9] numbered as in [9, Table 1]

Using a similar approach, we also verified that the corresponding problem in [7] has 4 real and 4 nonreal solutions.

We now turn to the second case. The fixing of a_0, d_0, α_0, and θ_0 yield the four constraints in Eqs. (15,16,17). Since

$$\mathbf{z}_3 = \begin{bmatrix} \sin\phi \sin\alpha_3 \\ \cos\phi \sin\alpha_3 \\ \cos\alpha_3 \end{bmatrix}, \quad \mathbf{v} = \begin{bmatrix} -a_3 \cos\phi - d_3 \sin\phi \sin\alpha_3 \\ a_3 \sin\phi - d_3 \cos\phi \sin\alpha_3 \\ -d - d_3 \cos\alpha_3 \end{bmatrix},$$

and $\mathbf{w}_3$ points in the direction of $\mathbf{z}_3$, the fixing of d and ϕ yield the constraints

$$\begin{bmatrix} \cos\phi & -\sin\phi & 0 \\ (d+\mathbf{v}^{(3)})\sin\phi & (d+\mathbf{v}^{(3)})\cos\phi & -\mathbf{v}^{(1)}\sin\phi - \mathbf{v}^{(2)}\cos\phi \end{bmatrix} \mathbf{w}_3 = 0.$$

As above, regeneration [19] starting from the witness set computed in Section 4 with general slices in $\mathbf{w}_1, \mathbf{w}_{21}, \mathbf{w}_3, \mathbf{v}$ yields 8 solutions verifying [7].

We use this setup to solve the corresponding problem in [7], namely

$$a_0 = d_0 = d = 2, \alpha_0 = \theta_0 = \phi = \pi/2.$$

Using quaternions, the 3 poses are

$$\begin{array}{l} \mathbf{q}_1 = \begin{bmatrix} -0.2241440446 & -0.1294095605 & 0 & -0.9659257802 \end{bmatrix}, \\ \mathbf{q}_2 = \begin{bmatrix} -0.270598115 & -0.270598115 & 0 & -0.9238794945 \end{bmatrix}, \\ \mathbf{q}_3 = \begin{bmatrix} 0 & 0.7071067812 & 0 & 0.7071067812 \end{bmatrix}, \\ \mathbf{p}_1 = \begin{bmatrix} 2.63397 & 8.78109 & 4.45096 \end{bmatrix}, \\ \mathbf{p}_2 = \begin{bmatrix} 4 & 8.24264 & 5.41421 \end{bmatrix}, \\ \mathbf{p}_3 = \begin{bmatrix} 6 & 6 & 6 \end{bmatrix}. \end{array}$$

Tracking the 8 solution paths took about one second using a single processing core compared with 70 hours reported in [7]. We again use `alphaCertified` to validate the solutions yielding 4 real and 4 nonreal solutions. Table 6 lists the real solutions using the variables of this article which correspond to the real solutions presented in [7, Table 2] using D-H parameters.

Solution	$\mathbf{v}$	$\mathbf{w}_1$	$\mathbf{w}_{21}$	$\mathbf{w}_3$
5	$\begin{bmatrix} -9.2333 \\ 14.653 \\ -2.2982 \end{bmatrix}$	$\begin{bmatrix} -0.21235 \\ 0 \\ 0 \end{bmatrix}$	$\begin{bmatrix} 4.4313 \\ -6.1108 \\ 2.2898 \end{bmatrix}$	$\begin{bmatrix} 1.4452 \\ 0 \\ 0.04667 \end{bmatrix}$
6	$\begin{bmatrix} -1.4595 \\ 1.1958 \\ -2.1357 \end{bmatrix}$	$\begin{bmatrix} 0.77721 \\ 0 \\ 0 \end{bmatrix}$	$\begin{bmatrix} -0.86986 \\ 1.6210 \\ -2.1025 \end{bmatrix}$	$\begin{bmatrix} 0.93937 \\ 0 \\ 0.087364 \end{bmatrix}$
7	$\begin{bmatrix} 39.179 \\ -66.268 \\ -1.9845 \end{bmatrix}$	$\begin{bmatrix} 0.029224 \\ 0 \\ 0 \end{bmatrix}$	$\begin{bmatrix} -34.190 \\ 43.851 \\ -24.800 \end{bmatrix}$	$\begin{bmatrix} 1.2950 \\ 0 \\ 0.00051168 \end{bmatrix}$
8	$\begin{bmatrix} -2.0000 \\ 2.0000 \\ -2.0000 \end{bmatrix}$	$\begin{bmatrix} 0.99996 \\ 0 \\ 0 \end{bmatrix}$	$\begin{bmatrix} -8.2051 \cdot 10^{-5} \\ 1.0000 \\ -1.7321 \end{bmatrix}$	$\begin{bmatrix} 1.0000 \\ 0 \\ -1.3567 \cdot 10^{-6} \end{bmatrix}$

Table 6: Real solutions for a 3-pose problem from [7] numbered as in [7, Table 2]

6. Conclusions

After developing a new formulation for the synthesis of 3R spatial chains for body guidance, we show how numerical algebraic geometry can be used

to solve several such synthesis problems. In particular, for the first time, this formulation and solving procedure shows that the 5-pose synthesis problem generically has 456 solutions. The output provides all the information needed to completely solve any particular 5-pose problem by using a parameter homotopy that starts from the solutions of our randomly chosen problem and continuously moves its five poses to the new ones. We used such a procedure to compute all solutions to the 5-pose problem from [10]. Our approach is much more efficient, producing full solution sets in 3 minutes (1 core) or 3 seconds (64 cores) compared to obtaining a partial solution set in 5 days.

When less than 5 poses are specified, the solution set of the synthesis problem consists of infinitely many points. We show how to use numerical algebraic geometry to compute a witness set for the solution set in all variables as well as a pseudowitness set for the projection of the solution set onto a subset of variables that suffice to define a unique 3R mechanism. This information can be used to solve other synthesis problems, including those formulated in terms of three or four poses and along with the specification of some of the Denavit-Hartenberg parameters. In particular, starting with the pseudowitness sets, we used the method of regeneration to verify the results in [7, 8, 9]. Moreover, in each of these cases we end up with a parameter homotopy that can solve such problems in seconds compared to previous reports requiring several days to get the same results.

The ability to rapidly and reliably solve all these variants of 3R synthesis problems will facilitate the design of any mechanism for body guidance that has a 3R chain between the guided body and ground.

With the complete solution to the 3R synthesis problems described here, the next open case in this direction is the synthesis of 4R spatial chains.

Acknowledgments

The synthesis problem for 3R spatial chains was posed as an open problem by the third author at the "Workshop on Software and Applications of Numerical Algebraic Geometry" which was supported in part by NSF DMS 1547743 and the Institute for Mathematics and its Applications (IMA). Research was supported in part by NSF ACI 1440607 and 1460032, Sloan Research Fellowship, and U.S. Army Research Office grant W911NF-15-1-0219 under the Young Investigator Program (YIP).

References

[1] A. M. Schoenflies, Geometrie der Bewegung in synthetischer Darstellung, B.G. Teubner, Leipzig, 1886.

[2] L. E. H. Burmester, Lehrbuch der Kinematik, Arthur Felix, Leipzig, 1888.

[3] P. Chen, B. Roth, Design equations for finitely and infinitesimally separated position synthesis of binary link and combined link chains, ASME J. Engineering for Industry 91 (1967) 209–219.

[4] J. M. McCarthy, Geometric Design of Linkages, Vol. 11 of Interdisciplinary Applied Mathematics, Springer, 2000.

[5] C. Innocenti, Polynomial solution of the spatial burmester problem, ASME J. Mech. Design 117 (1) (1995) 64–68.

[6] C. W. Wampler, A. P. Morgan, A. J. Sommese, Numerical continuation methods for solving polynomial systems arising in kinematics, ASME J. Mech. Design 112 (1) (1990) 59–68.

[7] E. Lee, C. Mavroidis, Solving the geometric design problem of spatial 3R robot manipulators using polynomial homotopy continuation, Journal of Mechanical Design 124 (2002) 652–661.

[8] E. Lee, C. Mavroidis, Geometric design of 3R robot manipulators for reaching four end-effector spatial poses, The International Journal of Robotics Research 23 (3) (2004) 247 – 254.

[9] E. Lee, C. Mavroidis, An algebraic elimination based algorithm for solving the geometric design problem of spatial 3R manipulators, in: Proc. ASME Design Eng. Tech. Conf.,Mech. & Robotics Conf., ASME, 2004.

[10] E. Lee, C. Mavroidis, J.-P. Merlet, Five precision point synthesis of spatial RRR manipulators using interval analysis, Journal of Mechanical Design 126 (2004) 842–849.

[11] J. Denavit, R. S. Hartenberg, A kinematic notation for lower-pair mechanisms based on matrices, Transactions of the ASME, Journal of Applied Mechanics 22 (1955) 215–221.

[12] D. J. Bates, J. D. Hauenstein, A. J. Sommese, C. W. Wampler, Numerically solving polynomial systems with Bertini, Vol. 25 of Software, Environments, and Tools, Society for Industrial and Applied Mathematics (SIAM), Philadelphia, PA, 2013.

[13] C. W. Wampler, A. J. Sommese, Numerical algebraic geometry and algebraic kinematics, Acta Numerica 20 (2011) 469–567.

[14] A. J. Sommese, J. Verschelde, C. W. Wampler, Advances in polynomial continuation for solving problems in kinematics, ASME Journal of Mechanical Design 126 (2) (2007) 262–268.

[15] C. W. Wampler, A. Morgan, Solving the 6R inverse position problem using a generic-case solution methodology, Mechanism and Machine Theory 26 (1) (1991) 91–106.

[16] A. Morgan, Solving polynomial systems using continuation for engineering and scientific problems, Vol. 57, SIAM, 2009.

[17] A. J. Sommese, C. W. Wampler, The Numerical solution of systems of polynomials arising in engineering and science, World Scientific, 2005.

[18] J. D. Hauenstein, A. J. Sommese, Witness sets of projections, Appl. Math. Comput. 217 (7) (2010) 3349–3354.

[19] J. D. Hauenstein, A. J. Sommese, C. W. Wampler, Regeneration homotopies for solving systems of polynomials, Math. Comp. 80 (273) (2011) 345–377.

[20] S. Smale, Newton's method estimates from data at one point, in: The merging of disciplines: new directions in pure, applied, and computational mathematics (Laramie, Wyo., 1985), Springer, New York, 1986, pp. 185–196.

[21] L. Blum, F. Cucker, M. Shub, S. Smale, Complexity and real computation, Springer-Verlag, New York, 1998, with a foreword by Richard M. Karp.

[22] J. D. Hauenstein, F. Sottile, Algorithm 921: alphaCertified: certifying solutions to polynomial systems, ACM Trans. Math. Software 38 (4) (2012) Art. ID 28, 20 pages.

[23] A. J. Sommese, J. Verschelde, C. W. Wampler, Symmetric functions applied to decomposing solution sets of polynomial systems, SIAM J. Numer. Anal. 40 (6) (2002) 2026–2046.

[24] D. A. Brake, J. D. Hauenstein, A. C. Liddell, Decomposing solution sets of polynomial systems using derivatives, in: G.-M. Greuel, T. Koch, P. Paule, A. Sommese (Eds.), Mathematical Software – ICMS 2016: 5th International Conference, Berlin, Germany, July 11-14, 2016, Proceedings, Springer International Publishing, Cham, 2016, pp. 127–135.

[25] J. D. Hauenstein, J. I. Rodriguez, Numerical irreducible decomposition of multiprojective varieties, arXiv:1507.07069 (2015).